GSA DATA REPOSITORY 2014350

Rainfall conditions, typhoon frequency, and contemporary landslide erosion in Japan

H. Saito[1,2], O. Korup[3], T. Uchida[4], S. Hayashi[4,5], and T. Oguchi[2]

[1]*College of Economics, Kanto Gakuin University, 1-50-1, Mutsuura-higashi, 236-8501, Japan*

[2]*Center for Spatial Information Science, The University of Tokyo, 5-1-5, Kashiwanoha, 277-8568, Japan*

[3]*Institute of Earth and Environmental Sciences, University of Potsdam, Karl-Liebknecht-Str. 24, Potsdam D-14476, Germany*

[4]*SABO Planning Division, National Institute for Land and Infrastructure Management, Asahi 1, 305-0804, Japan*

[5]*Present Affiliation: Chubu Regional Bureau, Ministry of Land, Infrastructure, Transport and Tourism, 2-5-1, San-no-maru, 460-8514, Japan*

Appendix DR1: Landslide Inventories

In Japan, the Ministry of Land, Infrastructure, Transport and Tourism (MLIT), prefectural and city governments have conducted detailed field survey of landslides for prevention against secondary disasters and for recovery from the disasters. They conducted the field investigation when the landslide induced any damage on human lives, house, and infrastructures, or if it can be thought that the landslide will cause damage on human lives, house, and infrastructures in near future due to small amount of rainfalls. MLIT collected results of these investigations as landslide inventories for making their policies and technical guidelines of landslide warnings (e.g., Osanai et al., 2010). These data comprise for each landslide the location; timing; rainfall conditions; lithological setting; general landslide type (i.e., shallow landslides, debris flows, rock slides, deep-seated slow-moving failures, and earthflows); landslide size (i.e., landslide volume, landslide area); damage (i.e., number of victims, damaged houses and infrastructures); reports on circumstances (i.e., possibility of secondary disasters, condition of access etc.) by surveyed engineers. Location, volume, and landslide type were measured and estimated in detailed field survey. The timing of each landslide was estimated from resident reports, hearing investigations, and reported infrastructure breakdown. Thus, if the landslide occurred in daytime, the accuracy of the reported landslide timing should be less than a few hours after each landslide occurrences. While, if the landslide occurred in night time, a maximum error might be around a half day.

However, some inventories might include errors. Thus, we carefully checked all reported location, timing, size of landslide and we excluded an inventory which might be included errors from our analysis. Moreover, some inventories had not complete information, since sometimes field survey was not effective to get a data about timing, landslide size and so on. So, we systematically filtered the total database of >10,000 entries, and limited our analysis to shallow landslides, debris flows, and rock slides (n = 4,744) that had complete listings of accurate location, volume, and timing.

Table DR1. Statistics of the most frequent landslide rainfall (freq., blue vertical lines in Fig. 2) and the highest volumetric landslide totals (vol., orange vertical lines in Fig. 2) for rainfall totals, duration, and mean and maximum intensity. Statistics are shown for all data; 1,000 random draws containing ~67% of the data each; a subset of the largest landslides (making up 1% of all data points); the dominant slope material and failure type; major lithology; and quartiles of population density (see Fig. S2). Data were calculated for each subset using multiple log-transformed bin widths from 0.05 to 0.2 [a.u.] at steps of 0.001 [a.u.], and are reported here as means and standard deviations.

Dataset		Total Rainfall (mm)	Mean Rainfall Intensity (mm/h)	Maximum Rainfall Intensity (mm/h)	Rainfall Duration (h)
All dataset	freq.	158.7 (± 14.7)	1.8 (± 0.1)	29.6 (± 4.4)	38.9 (± 6.5)
(n = 4,744)	vol.	1,066.9 (± 111.6)	10.5 (± 1.3)	29.2 (± 3.2)	103.7 (± 9.1)
Subset	freq.	156.1 (± 36.2)	2.0 (± 0.0)	32.3 (± 1.3)	51.2 (± 2.2)
(*)	vol.	1,284.5 (± 110.2)	12.0 (± 1.9)	32.6 (± 1.7)	127.6 (± 8.8)
Subset of largest landslides	freq.	299.7 (± 27.6)	4.3 (± 0.9)	27.3 (± 2.2)	82.2 (± 14.9)
(n = 48, 1% of all dataset)	vol.	1064.1 (± 96.6)	10.6 (± 1.3)	29.2 (± 3.0)	104.3 (± 9.1)
Shallow landslides	freq.	159.9 (± 15.4)	1.8 (± 0.2)	29.8 (± 3.3)	36.9 (± 5.4)
(n = 4,152)	vol.	307.5 (± 27.4)	5.5 (± 0.5)	51.5 (± 9.8)	974.1 (± 99.9)
Debris flows	freq.	312.5 (± 36.0)	2.5 (± 1.2)	32.1 (± 8.4)	50.5 (± 4.8)
(n = 510)	vol.	974.1 (± 99.9)	10.1 (± 1.4)	35.6 (± 3.4)	93.7 (± 8.5)
Rock slides	freq.	215.4 (± 71.8)	1.7 (± 0.5)	19.7 (± 2.5)	48.9 (± 6.7)
(n = 82)	vol.	1,151 (± 190.5)	11.1 (± 1.9)	28.8 (± 2.5)	104.1 (± 9.1)
Quaternary	freq.	153.7 (± 26.4)	1.6 (± 0.2)	23.3 (± 6.4)	34.6 (± 4.4)
(n = 1,503)	vol.	734.9 (± 76.8)	5.3 (± 0.5)	63.8 (± 5.8)	157 (± 14.2)
Sedimentary	freq.	147.0 (± 13.9)	2.0 (± 0.3)	20.7 (± 1.9)	34.9 (± 4.5)
(n = 898)	vol.	302.7 (± 26.5)	3.9 (± 0.4)	17.2 (± 1.5)	79.8 (± 7.0)
Accretionary Complex	freq.	167.8 (± 28.1)	1.8 (± 0.2)	30.1 (± 3.3)	29.4 (± 12.9)
(n = 718)	vol.	1,074.8 (± 107.7)	10.5 (± 1.3)	29.2 (± 3.2)	104.1 (± 9.1)
Volcanics	freq.	194.9 (± 20.2)	2.9 (± 0.5)	29.0 (± 3.5)	53.4 (± 6.1)
(n = 989)	vol.	764.8 (± 66.2)	8.9 (± 0.8)	28.0 (± 4.0	86.9 (± 7.9)
Plutonics	freq.	211.6 (± 13.3)	1.8 (± 0.2)	31.0 (± 3.3)	52.9 (± 4.7)
(n = 399)	vol.	292.8 (± 13.8)	5.0 (± 0.4)	53.7 (± 4.8)	60.2 (± 5.5)
Metamorphic	freq.	195.8 (± 57.2)	2.0 (± 0.3)	31.7 (± 6.4)	42.5 (± 6.6)
(n = 208)	vol.	388.4 (± 35.3)	4.4 (± 0.4)	57.0 (± 7.8)	89.4 (± 8.1)
0-81 people/km^2	freq.	159.8 (± 20.0)	1.7 (± 0.2)	29.5 (± 3.9)	51.6 (± 4.8)
(n = 1,195)	vol.	1,066.9 (± 111.6)	10.6 (± 1.3)	29.2 (± 3.2)	104.1 (± 9.1)
82-256 people/km^2	freq.	209.8 (± 23.0)	1.7 (± 0.2)	32.5 (± 3.2)	33.1 (± 7.1)
(n = 1,180)	vol.	750.6 (± 71.2)	8.5 (± 0.9)	28.6 (± 4.2)	94.4 (± 8.6)
257-1,103 people/km^2	freq.	159.4 (± 4.7)	1.8 (± 0.2)	24.5 (± 3.7)	32.4 (± 3.8)
(n = 1,184)	vol.	420.1 (± 85.6)	4.5 (± 0.4)	54.0 (± 20.7)	54.6 (± 22.3)
1,104-24,195 people/km^2	freq.	141.6 (± 20.6)	2.4 (± 0.3)	29.6 (± 6.5)	40.4 (± 3.9)
(n = 1,185)	vol.	331.9 (± 29.7)	8.8 (± 0.8)	86.0 (± 7.7)	38.6 (± 3.5)

* n = 1000 random subsets of two thirds of the landslide data

Table DR2. Recurrence intervals (yr, means and standard deviations) for the most frequent landslide rainfall (freq.) and the highest volumetric landslide totals (vol.) using a Gumbel (extreme-value type I) and a Generalized Extreme Value (GEV) distributions with jackknife fitting on a 34-yr time series of rain-gauge data recorded by the JMA at Owase and Abashiri stations from 1978 to 2011; N.D. = Not determined.

		return periods with Jackknif fitting (yr)			
	rainfall variables	Abashiri Gumbel	Abashiri GEV	Owase Gumbel	Owase GEV
total rainfall	158.7 (freq.)	23.1 (±4.4)	19.0 (±2.3)	1.0 (±0.0)	1.0(±0.0)
(mm)	1066.9 (Vol.)	N.D.	N.D.	43 (±3.9)	78.6 (±11.3)
max. intensity	29.6 (freq.)	41.5 (±8.2)	38.9 (±28.1)	1.0 (±0.0)	1.0 (±0.0)
(mm/h)	29.2 (vol.)	38.0 (±7.3)	35.7 (±23.3)	1.0 (±0.0)	1.0 (±0.0)
mean intensity	1.8 (freq.)	1.1 (±0.0)	1.0 (±0.0)	1.0 (±0.0)	1.0 (±0.0)
(mm/h)	10.5 (vol.)	19.1 (±3.7)	16.9 (±1.8)	1.5 (±0.0)	1.5 (±0.0)
duration	38.9 (freq.)	1.0 (±0.0)	1.0 (±0.0)	1.0 (±0.0)	1.0 (±0.0)
(h)	103.7 (vol.)	4.2 (± 0.2)	4.9 (±0.3)	1.2 (±0.0)	1.2 (±0.0)

Figure DR1. Estimated probability density of volumes of 4,744 rainfall-associated landslides mapped between 2001 and 2011 throughout Japan may be modelled by inverse power law: β_{IQR} is the negative power-law slope estimated from maximum likelihood, based on the interquartile range of recorded and ranked landslide volumes. β_{50} is the negative power-law slope based on the median of ranked landslide volumes. Data are binned for better legibility with bin widths of 0.2 of log-transformed landslide volume.

Figure DR2. Fraction of landslide number (gray curve) and average landslide volume (red curve) for (a) rainfall totals, (b) duration, and (c) mean and (d) maximum intensity. Bubble size scaled to average landslide volume per bin; bubble color reflects percentage of tropical cyclones out of total landslide-related rainfall events, with darker tones indicating higher contributions. Vertical lines are peaks of landslide-triggering frequency (blue) and total volume (orange), respectively (see Fig. 2). Black dashed lines are values at which landslides exceeding the median volume outnumbered smaller ones (see Figs. 3, DR6; not observed for rainfall duration); gray boxes encompass $\pm 1\sigma$.

Figure DR3. Log-binned frequency distributions of rainfall characteristics (solid gray line) and total mobilized landslide volume (dashed orange line) for selected subsets of the landslide data stratified by randomization, i.e. 1,000 random draws containing ~66% of the data each; dominant slope material and failure type; major lithology; and quartiles of population density. Bubble size scaled to total landslide volume per bin; bubble brightness scaled to percentage of tropical cyclones out of total number of landslide-rainfall events, with darker tones indicating higher fractions. Black circles outline most frequent rainfall characteristics associated with landslide reports. Vertical lines and gray boxes are means and error bars of +/- 2 σ for rainfall characteristics that were most frequent (blue), and related with the highest total landslide volumes (orange) in the study period, respectively.

Figure DR4. Log-binned frequency distributions of rainfall characteristics (solid gray line) and total mobilized landslide volume (dashed orange line). For data signatures see Fig. 2. Here we delimit individual rainfall events if separated by >12 h of no rain.

Figure DR5. Log-binned frequency distributions of landslide-triggering rainfall parameters (black), and all rainfall parameters (gray) that occurred between 2001 and 2011 across Japanese archipelago for (a) total rainfall (mm), (b) rainfall duration, and (c) mean and (d) maximum rainfall intensity (mm/h). Gray boxes encompass maximum range of 1-in-50-yr events defined by data from Abashiri and Owase stations (lower and upper boundary, respectively). Data are shown in the different x- and y-axes to represent the frequency distributions all rainfall event (gray plots).

Figure DR6. Log-binned frequency distributions of rainfall parameters and total landslide volumes below (dark gray lines), and above (light gray lines) the median volume for rainfall totals, duration, and mean and maximum intensity. Bubbles size scaled to total landslide volume

in each bin. Break lines represent values where the frequency of larger landslides surpasses that of small landslides; this is not evident in rainfall duration data (see Fig. 3 for full documentation.

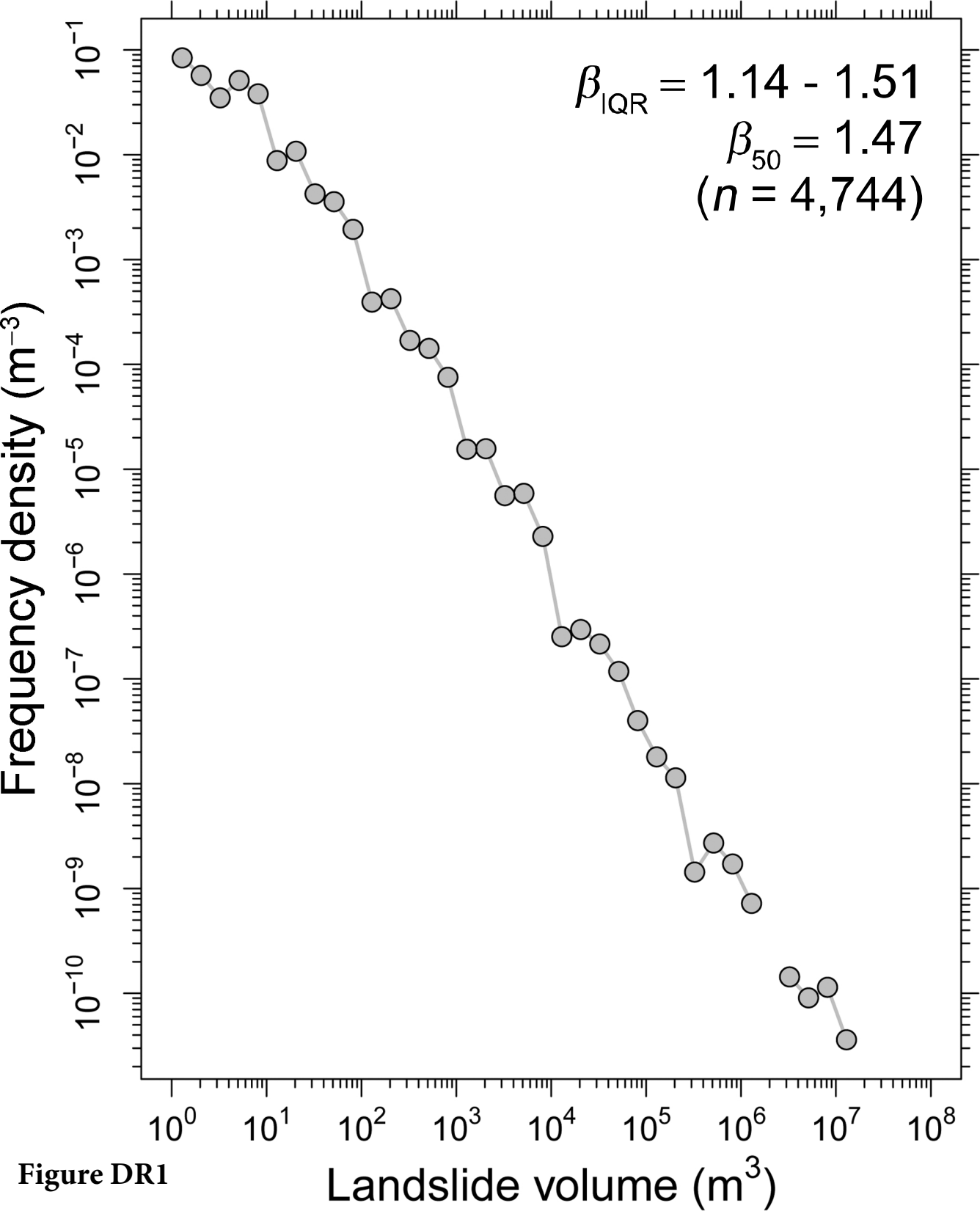
$\beta_{IQR} = 1.14 - 1.51$
$\beta_{50} = 1.47$
(n = 4,744)
Frequency density (m^{-3})
Landslide volume (m^3)
10^{-1}
10^{-2}
10^{-3}
10^{-4}
10^{-5}
10^{-6}
10^{-7}
10^{-8}
10^{-9}
10^{-10}
10^0
10^1
10^2
10^3
10^4
10^5
10^6
10^7
10^8

Figure DR1

Figure DR2

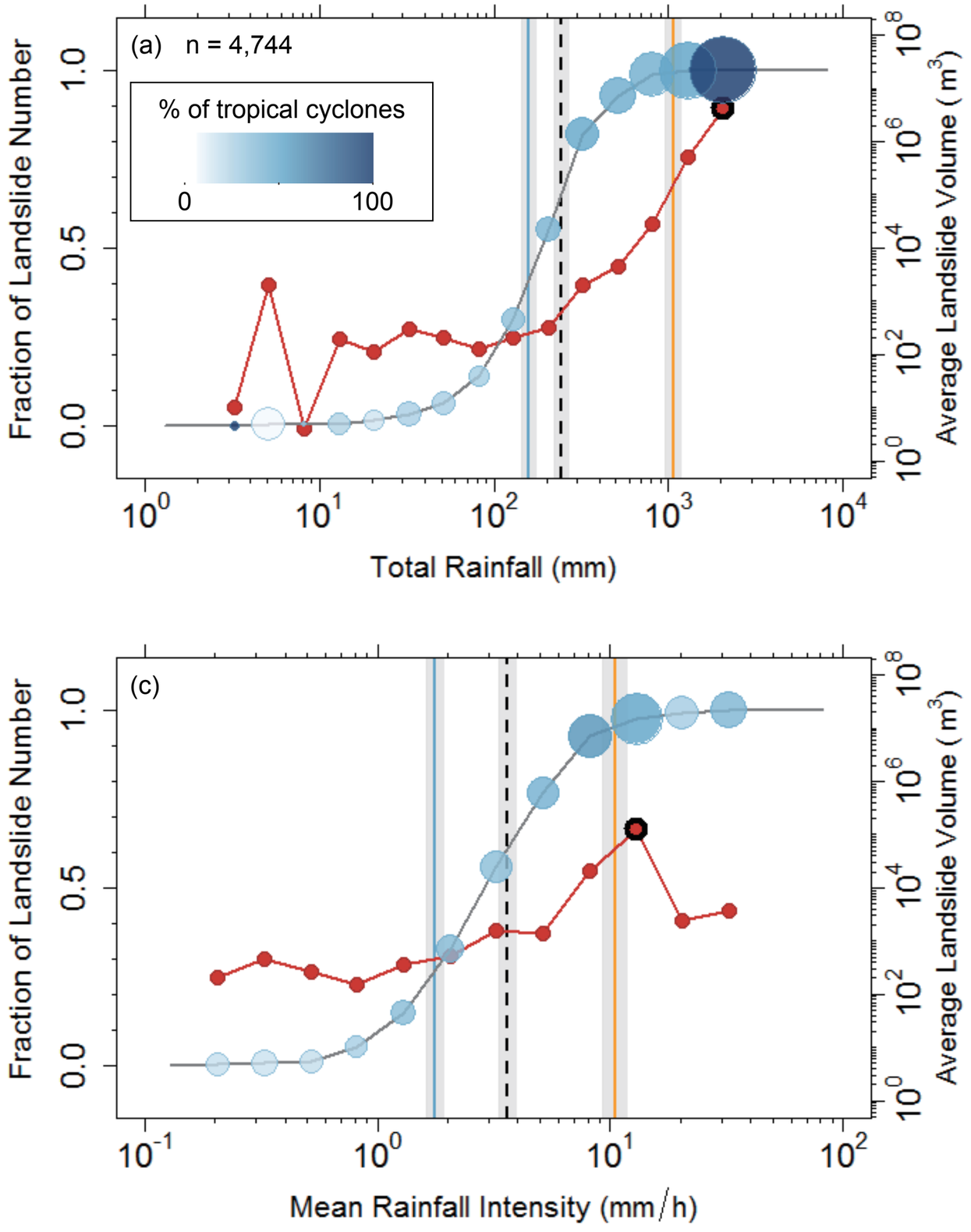
(a) n = 4,744
% of tropical cyclones
0
100
Fraction of Landslide Number
Average Landslide Volume (m3)
Total Rainfall (mm)

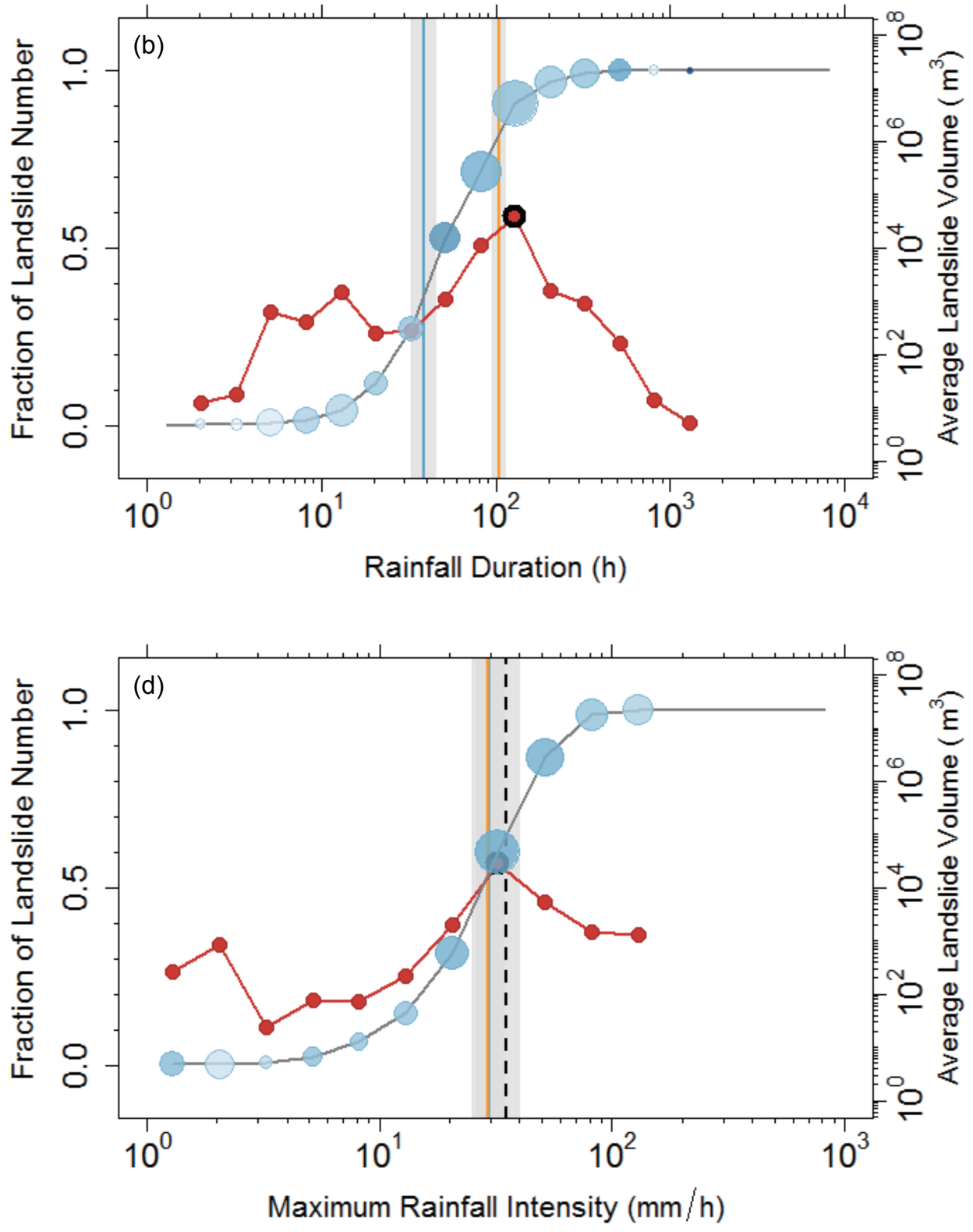
(b)
Fraction of Landslide Number
Average Landslide Volume (m3)
Rainfall Duration (h)

(c)
Fraction of Landslide Number
Average Landslide Volume (m3)
Mean Rainfall Intensity (mm/h)

(d)
Fraction of Landslide Number
Average Landslide Volume (m3)
Maximum Rainfall Intensity (mm/h)

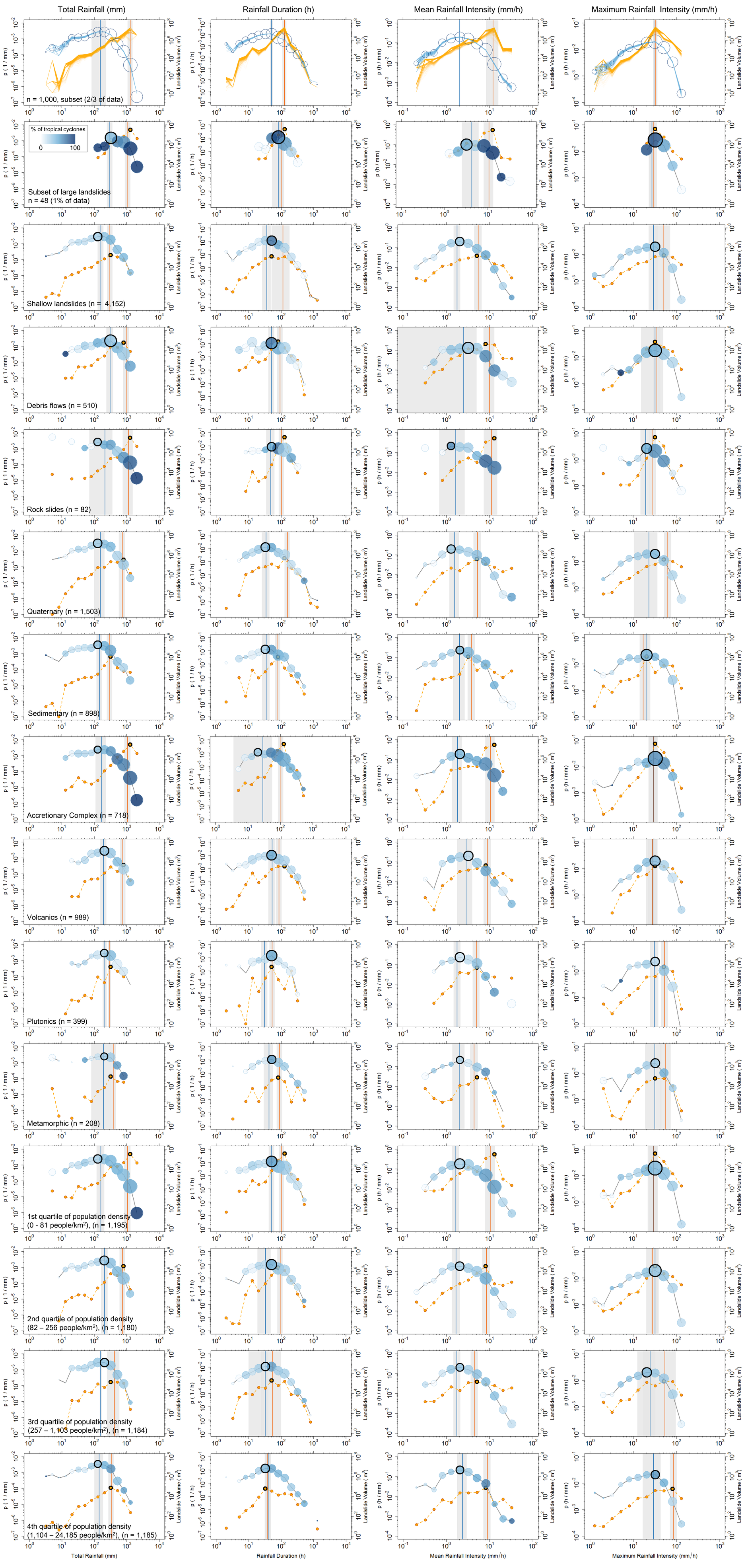
Total Rainfall (mm)
Rainfall Duration (h)
Mean Rainfall Intensity (mm/h)
Maximum Rainfall Intensity (mm/h)
p (1 / mm)
p (1 / h)
p (h / mm)
p (h / m)
Landslide Volume (m³)
n = 1,000, subset (2/3 of data)
% of tropical cyclones
0
100
Subset of large landslides
n = 48 (1% of data)
Shallow landslides (n = 4,152)
Debris flows (n = 510)
Rock slides (n = 82)
Quaternary (n = 1,503)
Sedimentary (n = 898)
Accretionary Complex (n = 718)
Volcanics (n = 989)
Plutonics (n = 399)
Metamorphic (n = 208)
1st quartile of population density
(0 - 81 people/km²), (n = 1,195)
2nd quartile of population density
(82 – 256 people/km²), (n = 1,180)
3rd quartile of population density
(257 – 1,103 people/km²), (n = 1,184)
4th quartile of population density
(1,104 – 24,185 people/km²), (n = 1,185)
Total Rainfall (mm)
Rainfall Duration (h)
Mean Rainfall Intensity (mm/h)
Maximum Rainfall Intensity (mm/h)

Figure DR3

Figure DR4

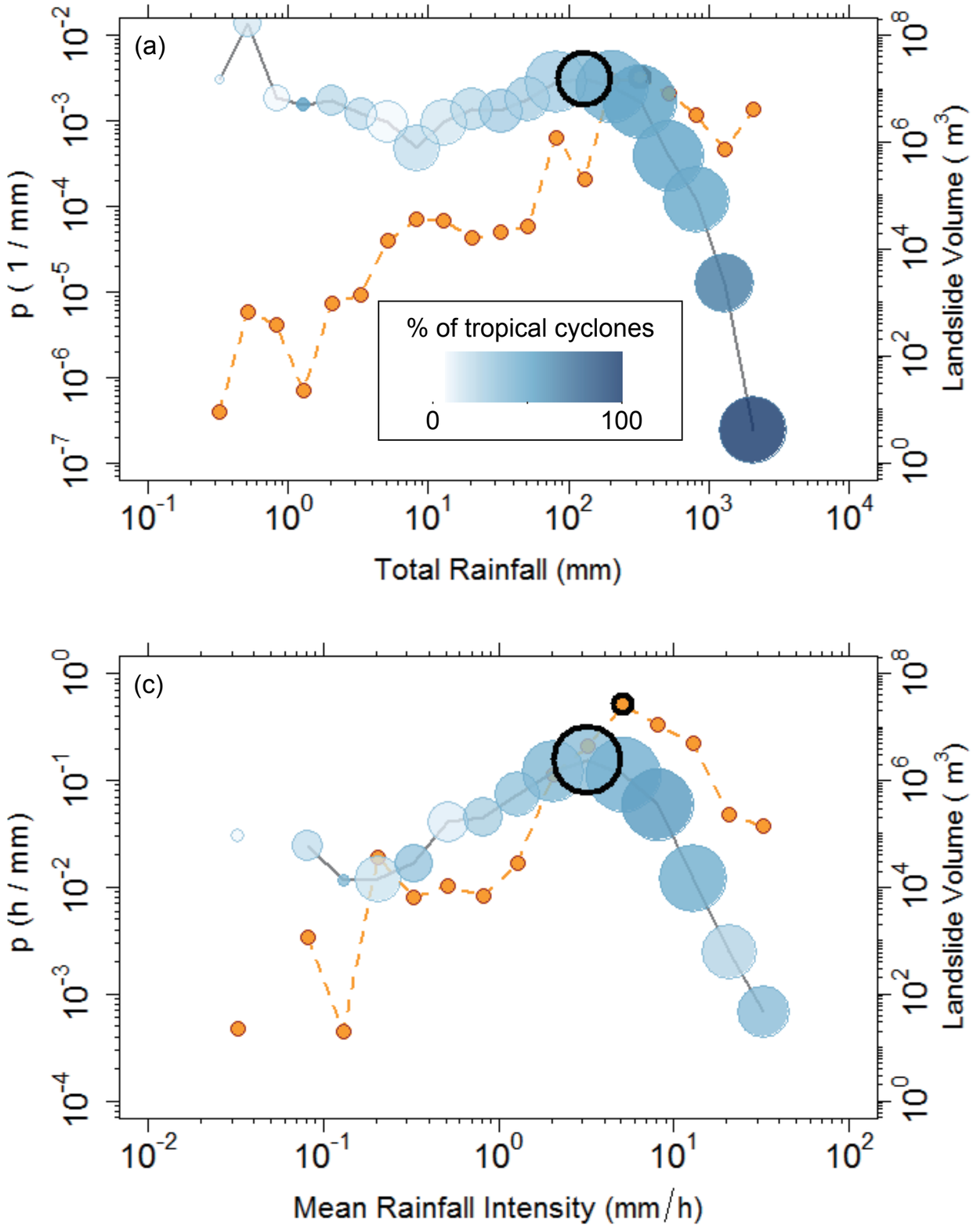
(a)
p (1 / mm)
Landslide Volume (m3)
Total Rainfall (mm)
% of tropical cyclones
0
100

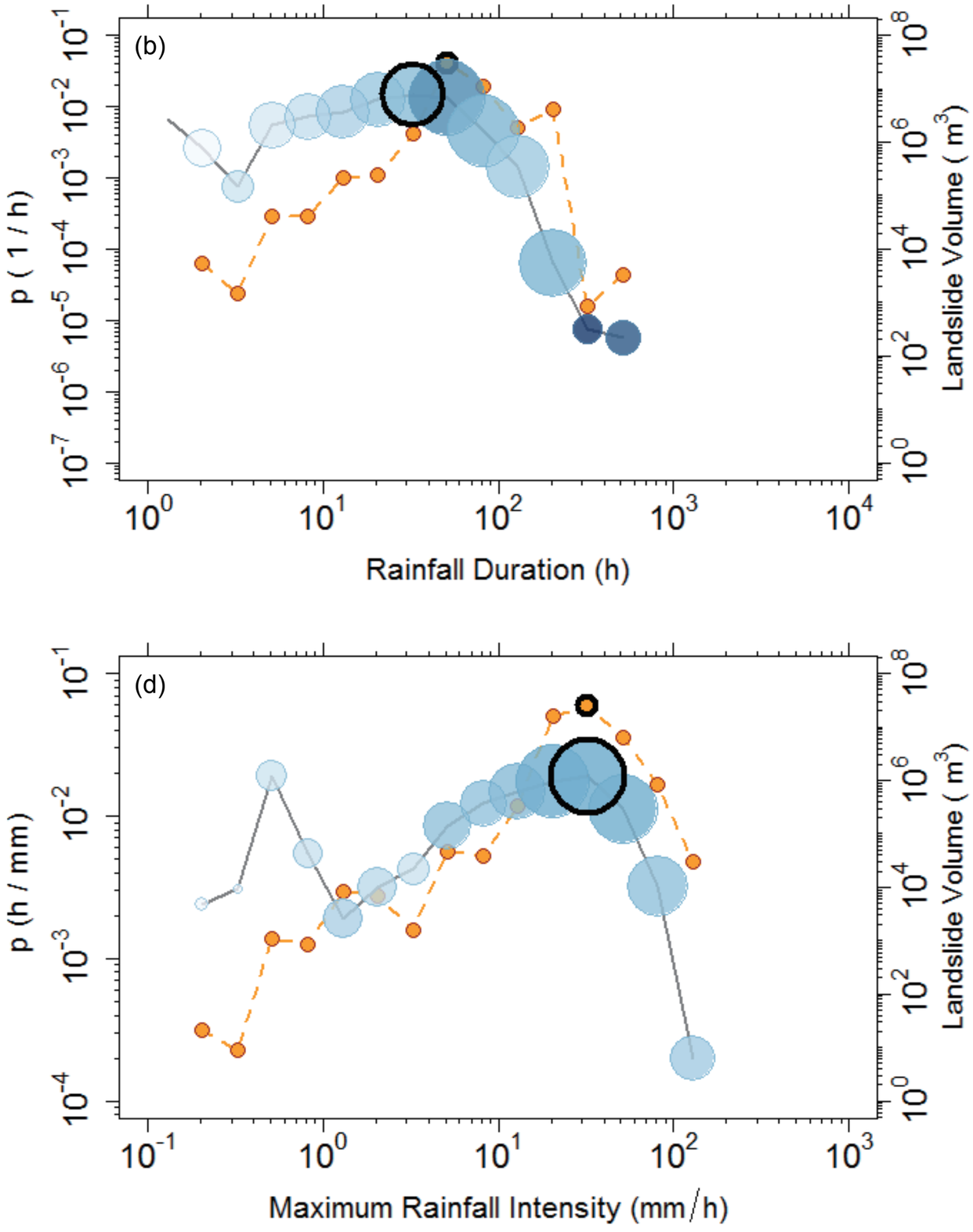
(b)
p (1 / h)
Landslide Volume (m3)
Rainfall Duration (h)

(c)
p (h / mm)
Landslide Volume (m3)
Mean Rainfall Intensity (mm/h)

(d)
p (h / mm)
Landslide Volume (m3)
Maximum Rainfall Intensity (mm/h)

Figure DR5

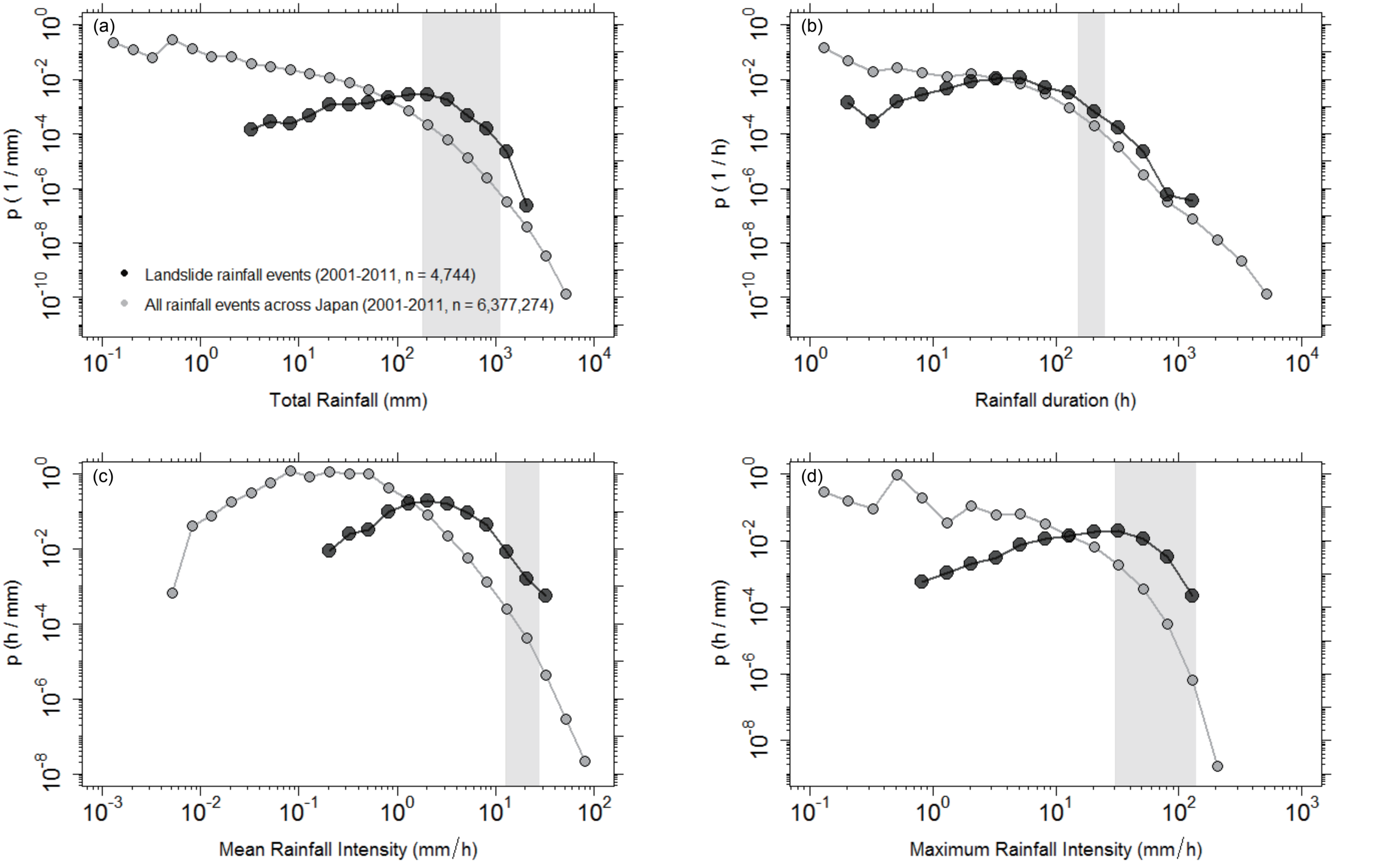
(a)
p (1 / mm)
Landslide rainfall events (2001-2011, n = 4,744)
All rainfall events across Japan (2001-2011, n = 6,377,274)
Total Rainfall (mm)
(b)
p (1 / h)
Rainfall duration (h)
(c)
p (h / mm)
Mean Rainfall Intensity (mm/h)
(d)
p (h / mm)
Maximum Rainfall Intensity (mm/h)

Figure DR6

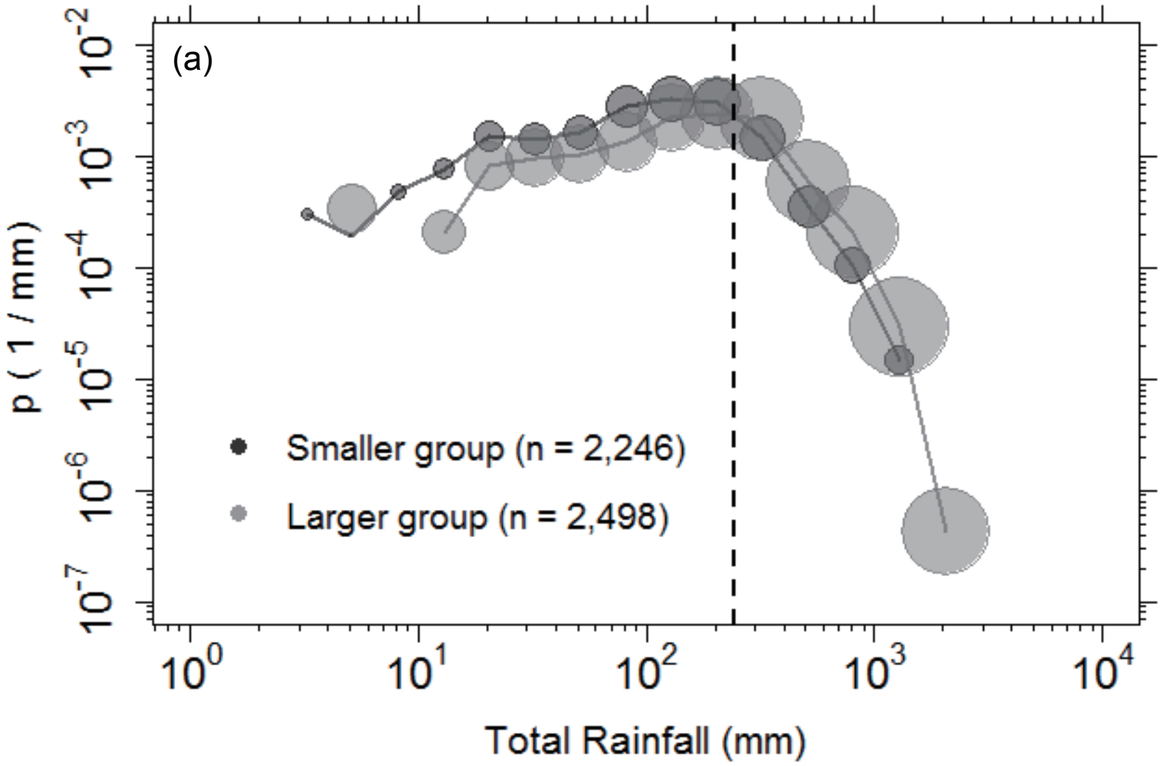
(a)
p (1 / mm)
Smaller group (n = 2,246)
Larger group (n = 2,498)
Total Rainfall (mm)

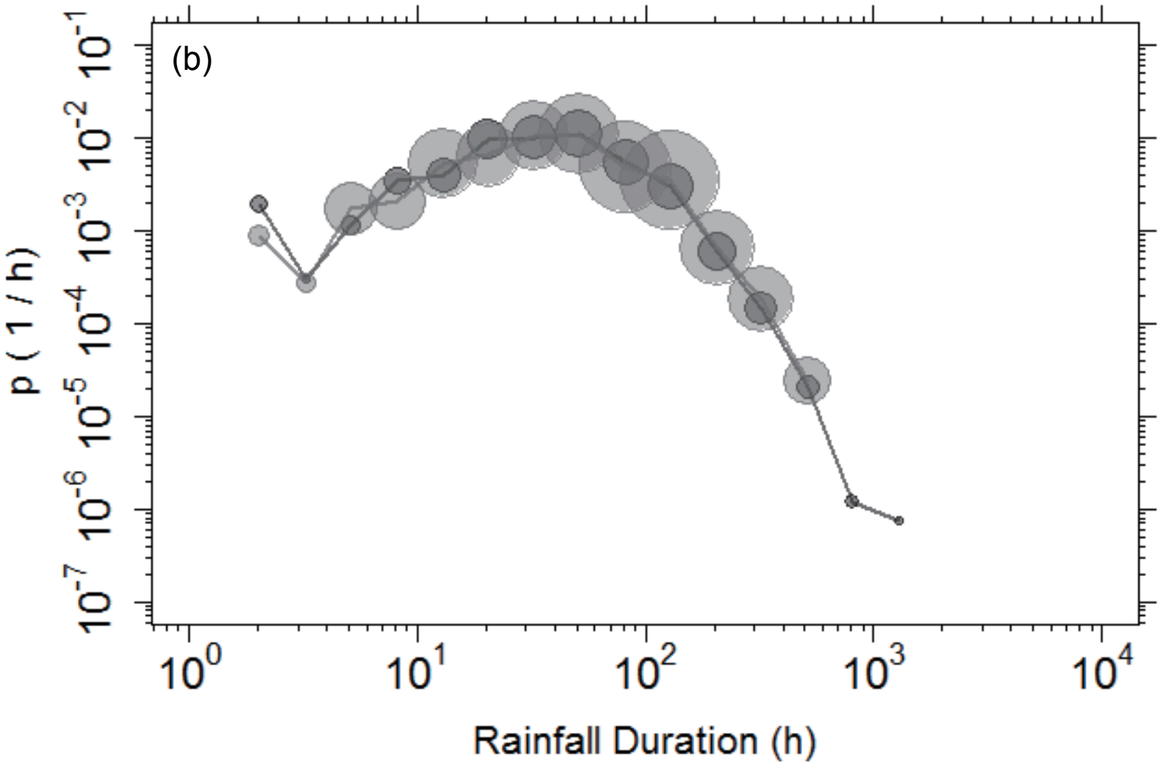
(b)
p (1 / h)
Rainfall Duration (h)

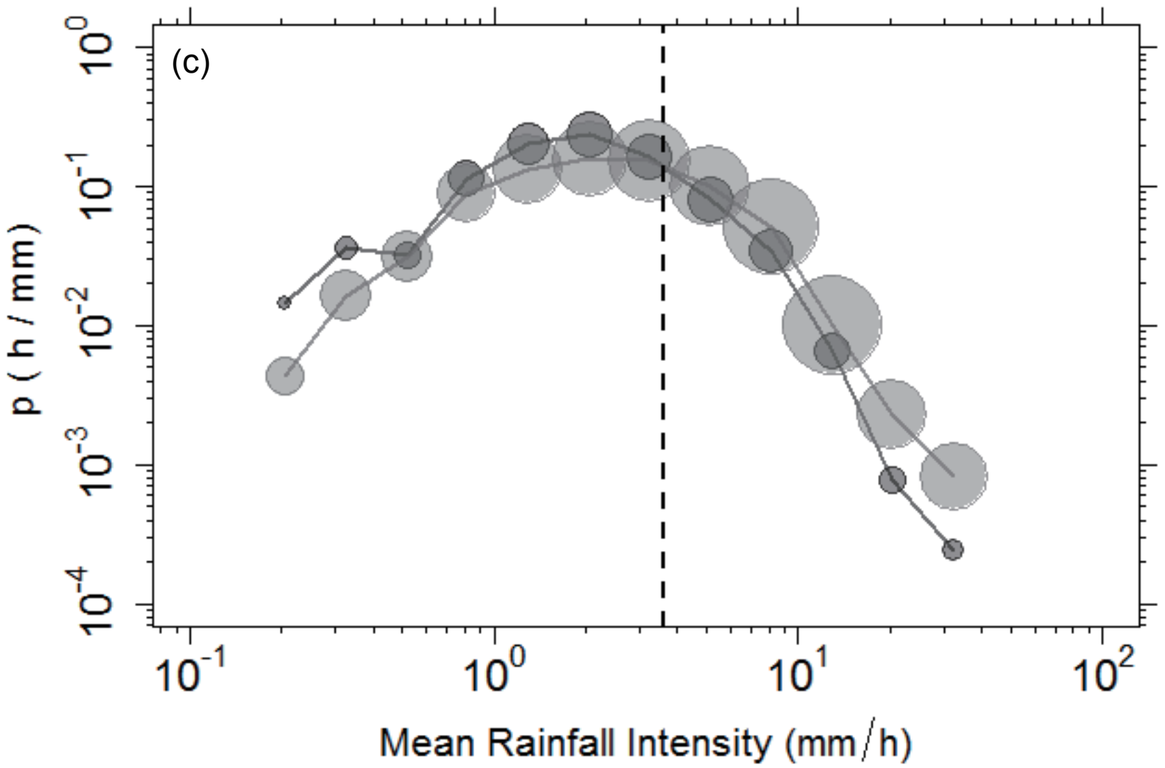
(c)
p (h / mm)
Mean Rainfall Intensity (mm/h)

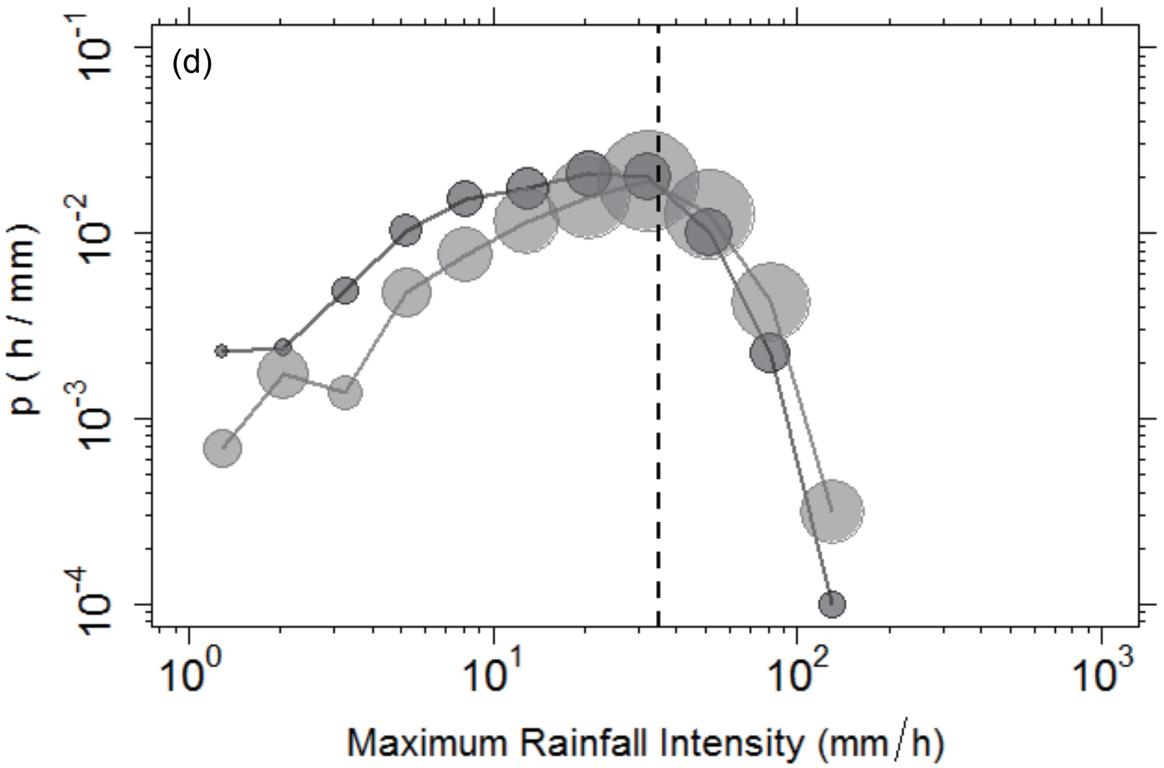
(d)
p (h / mm)
Maximum Rainfall Intensity (mm/h)